

## A fast open source muscle-driven shoulder model to study scapular dysfunctions

Ajay Seth<sup>1</sup>, Meilin Dong<sup>2</sup>, Ricardo Matias<sup>3</sup>, and Scott Delp<sup>1,2,4</sup>

<sup>1</sup>Bioengineering and <sup>2</sup>Mechanical Engineering Departments, Stanford University, United States

<sup>3</sup>Champalimaud Research, Champalimaud Centre for the Unknown, Lisbon, Portugal.

<sup>4</sup>Department of Orthopaedic Surgery, Stanford University, United States

Email: aseth@stanford.edu

### INTRODUCTION

Irregular scapular movement is indicative of shoulder dysfunctions such as subacromial impingement, rotator-cuff tears and other injuries [1]. A symptom of shoulder dysfunction is scapular dyskinesia [2] and particularly scapular winging [3], where the medial border of the scapula lifts off the thoracic surface. Anatomy textbooks [4] suggest that the serratus anterior muscle (SA) protracts and upward-rotates the scapula (in concert with trapezius), and SA weakness causes winging [2]. To investigate scapular dyskinesia requires models with the degrees of freedom (DOFs) and musculature of the scapula, currently unavailable in upper-extremity models [5,6]. In this study, we developed a model of the shoulder to examine how scapular muscles, including SA, are coordinated to achieve common upper-extremity tasks and the adaptations that are induced by weakness and ideal assistance.

### METHODS

We developed a model of the shoulder in OpenSim [7] (Fig.1) that combines a fast and accurate skeletal model of scapulothoracic kinematics [8] with muscle paths and architecture based on van der Helm et al. [9] adjusted to produce moment arms bounded by measurements from cadaver experiments [10]. Continuity of muscle moment arms was verified over the full range-of-motion of the model.

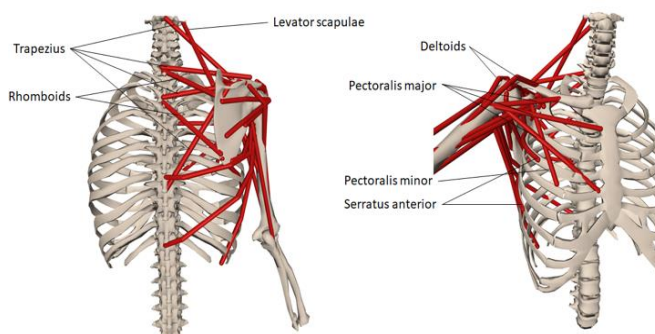


**Fig 1:** Musculoskeletal model of the shoulder and the muscles that control the scapula.

To test the model, we collected upper-extremity kinematics and muscle surface EMG using

Ascension 3D trakSTAR (Ascension Technology Corp, USA) and Biotell 99 (Glonner Electronic GmbH, Germany) systems. We collected three trials of shoulder shrugging and forward flexion with (denoted by '+') and without a 2kg hand-held weight for a total of 12 trials. Model scaling and inverse kinematics were performed in OpenSim to compute model joint angles. Computed muscle control (CMC) [11] was used to generate muscle-driven simulations that tracked joint angles. To validate the simulations we used muscle on/off timings computed from raw EMG signals [12]. To understand the contribution of individual muscles to shoulder movements, we calculated the work done by muscles.

We applied an ideal assist strategy to test its effects on muscle coordination and work during shoulder flexion tasks and a wall-push test typical of a clinical exam [3]. An ideal torque actuator was applied to the winging DOF to test that SA opposes winging [2]. The wall-push test was simulated with the humerus flexed at 90° and the elbow extended and locked. An external force was applied at the wrist along the long-axis of the forearm and the force was ramped from 0 to 550N. Finally, to test if assistance could compensate for SA weakness (e.g. due to brachial nerve palsy), we limited SA activity to a maximum of 10%, in the weakened case.

### RESULTS AND DISCUSSION

Muscle-driven simulations were generated in tractable times (Table 1) and estimated muscle controls from static optimization (SO) and CMC were used to perform forward dynamic (FD) simulations. Simulated muscle activity agreed with EMG on-off timings (e.g. Fig 2).

**Table 1.** Compute vs. real time ratio (compute/real) by task. Lower values are faster. \*CMC terminated early.

	SO	CMC	FD	Saul <sup>[6]</sup> CMC
<b>Shrug</b>	82	374	15	N/A
<b>Shrug+</b>	68	389	18	N/A
<b>Flex</b>	99	614	13	6689*
<b>Flex+</b>	93	347	18	1902*
<b>Push</b>	2	307	12	1192

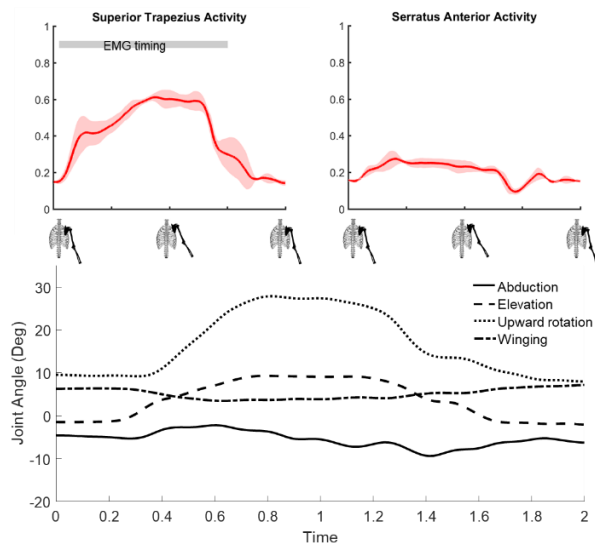


**Fig 2:** Muscle-driven simulation of a shoulder shrug. Top row are model muscle activations and bottom are scapulothoracic DOFs during the shoulder shrug.

The simulated shoulder shrug shows that the model can elevate and rotate the scapula independent of humerus elevation (Fig 2, bottom). The total work done by the top four active muscles (Table 2) indicate that shrug work is done mainly by superior trapezius. In flexion, SA and superior trapezius work together to upward-rotate the scapula while the deltoids elevate the humerus with respect to the scapula.

**Table 2.** Total positive work (J) done by muscles during the elevation phase of the shrugging and flexion tasks.

	Serratus anterior	Trapezius	Deltoids	Levator scapulae
<b>Shrug</b>	0.0	3.7	0.3	0.0
<b>Shrug+</b>	0.0	7.0	0.4	0.1
<b>Flex</b>	9.2	8.0	11.9	1.0
<b>Flex+</b>	17.3	12.3	21.8	1.7

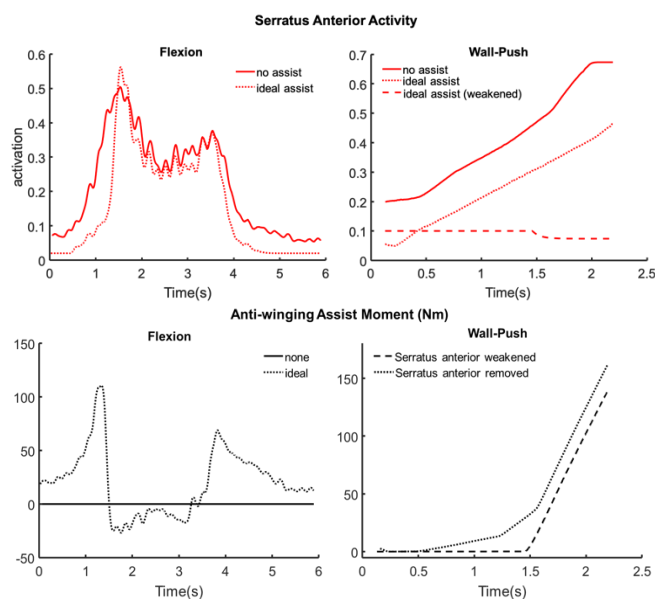


**Fig 3:** The effect of ideal anti-winging assist on SA activation during flexion with 2kg weight and wall-push tasks (top row). Ideal assist moments applied during flexion and wall-push (bottom row).

Ideal anti-winging assist had little effect on SA activity (Fig. 3 top left) and muscle work during forward flexion, with and without weight. During the wall-push test, ideal assist systematically reduced SA activity and could perform the test with SA weakened (Fig. 3 top right). Although both activities used assistance exceeding 100Nm (Fig. 3 bottom), the flexion tasks could not be performed in the weakened case, even with unlimited anti-winging assistance. These results are consistent with experiments indicating SA plays multiple roles in shoulder movement [13]. In flexion, inferior SA and superior trapezius work together to upward-rotate the scapula, which could not be achieved without this force couple. In the wall-push test, SA, particularly its superior and medial bundles, acts to oppose winging, which we showed could be compensated for by anti-winging assistance. Indeed, in the case of assistance, we see an increase in pectoralis major activity and force, suggesting that the balance of SA and pectoralis muscles to control winging limits the pushing force.

## CONCLUSIONS

In this study we developed a musculoskeletal model of the shoulder that includes the scapular DOFs and the musculature to control them. Model simulation time is tractable and faster than that of a popular upper-extremity model [6] that excludes scapular DOFs and muscles. Muscle-driven simulations mechanistically demonstrate, for the first time, the dual role of SA to do work in upward-rotating the scapula and to constrain the scapula against winging. We demonstrated how ideal anti-winging assistance can compensate for SA weakness, which highlights the clinical and rehabilitation utility of the model to simulate cause-and-effect relationships in the human shoulder.

## REFERENCES

1. Struyf F, et al. *Scand J Med Sci Sports* **21**:352, 2011.
2. Kibler WB and McMullen J. *J Am Acad Orthop Surg* **11**:142, 2003.
3. Martin RM & Fish DE, *Curr Rev Musculoskelet Med* **1**:1, 2008.
4. Gray H, *Anatomy of the human body*, 20th ed. 1918.
5. Chadwick E, et al. *IEEE Trans Biomed Eng* **61**(7):1947, 2014.
6. Saul KR, et al. *CMBBE* **18**:1445, 2015.
7. Seth A, et al. *Plos Comp Biol* **14**:e100622, 2018.
8. Seth A, et al. *PLoS ONE* **11**:e0141028, 2016.
9. Van der Helm FC, et al. *J Biomech* **25**:129, 1992.
10. Ackland DC, et al. *J Anatomy* **213**:383, 2008.
11. Thelen DG and Anderson FC. *J Biomech* **39**(6):1107, 2006.
12. Li X, *Ann Biomed Eng* **35**(9):1532, 2007
13. Ekstrom RA, et al. *JOSPT* **34**(5):235, 2004.